Available online at www.sciencedirect.com
SCIENCE DIRECT®
International Journal of Heat and Mass Transfer 49 (2006) 3156–3166
International Journal of HEAT and MASS TRANSFER
www.elsevier.com/locate/ijhmt

Temperature fluctuation at twin cavity in nucleate boiling—wavelet analysis and modelling

R. Mosdorf [a,*], M. Shoji [b,1]

[a] Faculty of Computer Science, Bialystok University of Technology, 15-351 Bialystok, ul. Wiejska, Poland
[b] National Institute of Advanced Industrial Science and Technology (AIST Tsukuba), Namiki 1-2-1, Tsukuba, Ibaraki 305-8564, Japan

Received 20 July 2005
Available online 4 April 2006

Abstract

In the paper the wavelet analysis of heating surface temperature fluctuation at the artificial cavities in nucleate boiling has been carried out. It has been shown that depending on distance between cavities the process of bubbles departure from twin cavity can synchronize and create the unified conditions for heat transfer around the cavities. It has been found that synchronization of interacting cavities leads to decrease in mean frequency of bubbles departure. The new concept of promotion or inhibition of interacting cavities has been defined based on the wavelet analysis. Two-dimensional boiling field was approximated and modeled using CML method. Two mechanisms of interaction between bubble columns have been considered: the thermal and hydrodynamic ones. The simulation shows that thermal interaction between two cavities and bubble columns leads to deactivation of neighboring cavity whereas the hydrodynamic interaction sustains the activity of neighboring cavity.

Keywords: Pool boiling; Wavelet analysis; Nucleation site interaction; CML method

1. Introduction

Despite of the extensive study of boiling during the past over 50 years, mechanisms of nucleate boiling are still far from being fully understood due to the extreme complexity of the phenomena. Among the sub-processes in nucleate boiling phenomena, the most important one may be the nucleation site problem [1].

Some researchers have already investigated the nucleate boiling heat transfer characteristics, the bubble behaviors and the surface temperature fluctuation [2,9,10,13,15]. The relations between the bubble behaviors and the cavity spacing, S/D, have been studied experimentally by Chekanov [3], Calka and Judd [4], Gjerkeš and Golobic [5]. Several authors have studied the heat transfer characteristics of the artificial boiling surfaces with multiple cavities aiming applications to the cooling of highly integrated electronic devices [6,7]. Recently, by employing twin cavities, Zhang and Shoji [8] have investigated the mechanism of nucleation sites interaction. Mosdorf and Shoji [12] apply the nonlinear analysis to investigate the nucleation site interaction.

During the neighboring cavities interaction the temperature changes in time are very complicated because of complex correlation between the different sub-processes occurring in nucleation boiling such as: heat transfer (in liquid and heating surface), phase changes, different kinds of bubbles coalescence, contact behaviors and liquid flow around the bubbles. The neighboring cavities interact through the heat transfer in liquid and heating surface, by liquid flow around the bubbles and different mechanisms of coalescence [8]. All mechanisms of interaction are characterized by different frequencies of temperature changes. The frequency analysis of temperature changes at neighboring cavities may allow us to better understand

* Corresponding author. Tel.: +48 85 7469050; fax: +48 85 7469057.
E-mail addresses: mosdorf@ii.pb.bialystok.pl (R. Mosdorf), shoji.m@aist.go.jp (M. Shoji).
[1] Tel.: +81 29 861 7053; fax: +81 29 861 7053/7275.

0017-9310/$ - see front matter © 2006 Elsevier Ltd. All rights reserved.
doi:10.1016/j.ijheatmasstransfer.2006.02.010

Nomenclature

a	thermal diffusivity
C	correlation coefficient
Cov	covariation
D	bubble departure diameter
F	Fourier power spectrum
f	frequency
N	number of samples
q	heat flux
s	scaling parameter
S	distance between the cavities
T	temperature
t	time, time index
t'	time translation
W	wavelet power spectrum
x	coordinates

Greek symbols

σ	standard deviation
ω	frequency
η	nondimensional time
Ψ	translated version of based wavelet $\Psi_o(\eta)$

Subscripts

f	frequency
cf	phase change
k	frequency number
n	sample number
o	for $x = 0$
t	time index
t	time

Superscripts

l	left cavity
r	right cavity

the mechanisms of interaction, including understanding the role of process responsible for interaction.

In the paper the wavelet analysis of temperature fluctuation of heating surface at the artificial neighboring cavities has been carried out. The wavelet power spectrum has been used to analyze the temperature fluctuation at single cavity and at twin cavities for different distances between them. The correlation coefficients of temperature changes and wavelet spectrum at twin cavities have been calculated and discussed.

In the present study, the two-dimensional boiling field was approximated and modeled using CML method. Two mechanisms of interaction between bubble columns—the thermal and hydrodynamic ones—have been discussed.

2. Experimental setup

A 15 mm × 15 mm and 200 μm thick silicon disk with artificial nucleation sites was set as a test boiling surface inside the chamber filled with distilled water. Schematic view of the whole experimental setup is shown in Fig. 1. In the experiment, vicinity of the manufactured cavity was heated by Nd-YAG laser irradiation (wavelength: 1064 nm) from the bottom side of the test disk. The size of laser spot was 12 mm in diameter. The bottom surface of the disk was black oxide finished in order to improve absorptivity of the input laser and emissivity from the surface. Temperature fluctuation just under the artificial cavity were recorded by radiation thermometer with spatial resolution of 120 μm, temperature resolution of 0.08 K and time resolution of 3.0 ms. The corresponding bubbling status was recorded by high-speed video camera with the

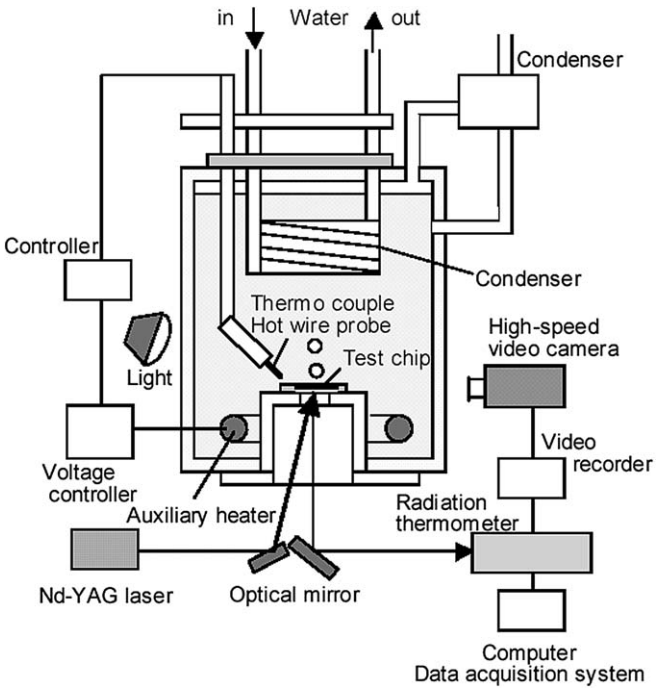

Fig. 1. Experimental apparatus.

rate of 1297 frames/s. In this way, it was possible to measure temperature time series of cavity vicinity without any physical contact to the disk surface. The power of Nd-YAG laser was controlled to vary the heat input to the disk surface and was monitored by photo detector throughout the experiment. Working fluid was distilled water at atmospheric pressure under saturated pool boiling condition. Acrylic fence was set inside the chamber to

avoid effect of bubbling from auxiliary heater, which was activated during the experiment to maintain saturated boiling condition.

To investigate the nucleation sites interaction, the silicon surface with twin cylindrical nucleation sites was used. The nucleation sites of 10 μm in diameter and 80 μm in depth was applied. The spacing, S, between two nucleation sites, was changed from 1 to 8 mm. As the size of the departing bubble without interference, D, was approximately 2.4 mm in diameter, the spacing employed corresponds to the spacing-to-bubble diameter ratio, S/D, from 0.4 to 3.3. In the present paper the time series of temperature fluctuation at twin cavity for $q = 26.5\ \mathrm{W/m^2}$ has been analyzed using the wavelet spectrum and correlation coefficient. The results of analysis has been compared with analysis of temperature fluctuation at single cavity for $q = 34.4\ \mathrm{W/m^2}$.

3. Comments about the cavities interaction

The experimental data collected from artificial twin cavities has been analysed in papers [8,12,16]. In the paper [8] the average bubble departure frequency from two artificial cavities for different dimensionless cavity spacing S/D has been calculated. For $S/D < 1.5$ the frequency of bubble departure reach up to 130 Hz for $q = 26.5\ \mathrm{kW/m^2}$. In this region, the frequency decreases together with increase of dimensionless cavity spacing, S/D. The frequency reaches the minimum of 50 Hz for $S/D = 1.5$. In the region, $2 < S/D < 3$, the mean frequency reaches the next maximum equal to 80 Hz for $S/D = 2.5$. For maximum investigated dimensionless cavity spacing $S/D = 3.3$ the mean frequency reaches 40 Hz. The mean frequency of bubble departure against spacing S/D has been shown in Fig. 6b.

Based on the comprehensive observation and analysis [8], three significant effect factors of nucleation site interaction have been found out: hydrodynamic interaction between bubbles, thermal interaction between nucleation sites, and horizontal and declining bubble coalescences. The concept of promotion and inhibition of cavities based on increase or decrease in mean frequency has been discussed in paper [8].

The nonlinear analyses carried out in the paper [12] allow us to distinguish two mechanisms of interaction between neighbouring nucleation sites: first of them of hydrodynamic character, occurring over the heating surface and the other one of thermal character, occurring inside the heating surface. The interaction through the liquid (coalescence and hydrodynamic interaction) increases the frequency of bubble departure (promotes the growing bubble to depart). It happens for bubbles spacing, $S/D = 0.63$ and $S/D = 2.5$. In these cases the process of bubbles departure becomes more predictable.

It has been found out [12] that the interaction between nucleation sites through the liquid stabilizes the process of bubble growth and its departure. The thermal interaction destabilizes this process.

4. Methods of analysis of frequency of temperature changes at cavity

The frequency of bubble departure from single cavity, as well as from twin cavities is not constant and changes in time. Two interacting cavities and departing bubbles play the role of generators of thermal waves within liquid and heating surface. It is well known that the amplitude of temperature changes is dumped depending on the frequencies of temperature changes and distance from cavity. The rate of dumping of temperature oscillations in half infinity body, when on the one side of body the temperature changes with frequency, f, and amplitude, T_0, can be estimated by the following formula [18]:

$$\frac{T}{T_0} = \pm \mathrm{e}^{-\sqrt{\frac{\pi f}{a}}x} \tag{1}$$

For silicon and $f = 30$ Hz the amplitude, T_0, decreases 100 times at distance of $x = 4.3$ mm. For $f = 5$ Hz this distance is equal to 10 mm. Therefore, it has been assumed that temperature fluctuation with high frequencies, measured at cavity, are caused by dynamic of bubbles growth at cavity, but temperature changes with low frequencies are the consequence of changing the condition of heat transfer around the cavities and departing bubbles.

The Fourier transformation allows us to represent time-domain data in the frequency domain. The Fourier power spectrum answers the question which frequencies contain the signal power. The answer has the form of a distribution of power values as a function of frequency. In the frequency domain, this is the square of Fourier transformation magnitude. The power spectrum can be computed for the entire signal at once or for segments of the time signal. For the measurement data in the form of discrete series T_n the Fourier transformation has a following form:

$$F_k = \sum_{n=0}^{N-1} T_n \mathrm{e}^{-j\frac{2\pi}{N}kl} \tag{2}$$

In this case the power spectrum is defined as $|F_k|^2$.

In Fig. 2a it has been shown the example of Fourier power spectrum of temperature fluctuation under the single cavity. The Fourier power spectrum identifies two main frequencies of temperature changes: 34 and 24 Hz. These frequencies correspond to frequencies of bubbles departure. The Fourier power spectrum do not allow us to identify the frequencies changes in time. This problem can be analyzed using the windowed Fourier transformation [11,14] but this is an inaccurate method for localizing time–frequency. The wavelet analysis is free from this inaccuracy, it is a tool for analyzing the localized variations of power spectrum within the time series T_n, with equal time spacing δt [11,14].

The continuous wavelet transformation of a discrete sequence T_n is defined as the convolution of T_n with a scaled wavelet Ψ [11,14]:

$$W(t,s) = \sum_{t'=0}^{N-1} T_{t'} \Psi * \left[\frac{(t'-t)\delta t}{s}\right] \tag{3}$$

where (*) indicates the complex conjugate.

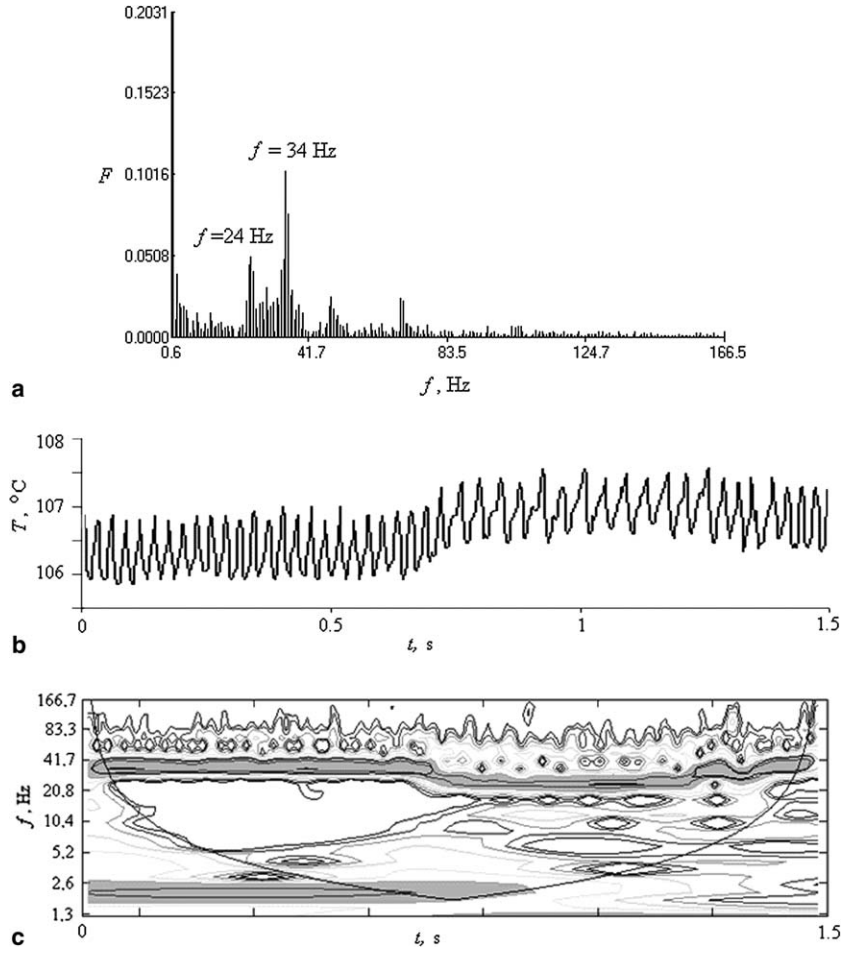

Fig. 2. Example of data analysis under the single cavity. (a) The power spectrum of temperature fluctuation under the single cavity, (b) the temperature fluctuation under the single cavity, (c) the wavelet power spectrum of temperature fluctuation under single cavity. $q = 34.4\ \mathrm{kW/m^2}$. (Wavelet software was provided by Torrence and Compo, and is available at URL: http://paos.colorado.edu/research/wavelets/, [11,14].)

Because the wavelet function $\Psi_o(\eta)$ is in general complex, the wavelet transformation $W(t,s)$ is also complex. The wavelet power spectrum is defined as: $|W(t,s)|^2$ [11,14].

During the analysis the Morlet wavelet has been used as the based wavelet. The Morlet wavelet has a form [11,14]

$$\Psi_o(\eta) = \pi^{-1/4} e^{i\omega_o \eta} e^{-\eta^2/2} \tag{4}$$

where ω_o—nondimensional frequency, in the paper it is equal to 6 [11,14].

In Eq. (3), the parameter s assigns the frequency whereas the parameter t identifies the time around which the assigned frequencies are investigated. The wavelet power spectrum is presented in the form of three-dimensional map, where the horizontal axis shows the values of parameter t, while the vertical axis shows the values of parameter s (frequency). The values of wavelet power spectrum $|W(t,s)|^2$ are presented as an altitude. The wavelet power spectrum allows us to observe the changes in time of each frequency power. In Fig. 2c, the contour plot of the wavelet power spectrum for temperature fluctuation at the single cavity has been presented. The areas containing the highest value of $|W(t,s)|^2$ are filled with a gray color. The investigated temperature changes at single cavity have been shown in Fig. 2b.

The changes of location of maximum values of $|W(t,s)|^2$ identify the changes in time of the dominant frequency. The Fourier power spectrum, shown in Fig. 2a, identifies two dominant frequencies of temperature changes: 24 and 34 Hz. The wavelet power spectrum shows in what period of time of the temperature time series these frequencies appear. We can notice that in time period from 0.7 to 1.3 s the dominant frequency is equal to 24 Hz. In other time the dominant frequency is equal to 34 Hz.

The existence of neighboring nucleation sites makes that the temperature changes become more complex in comparison with the temperature changes at the single nucleation site. In Fig. 3, it has been shown the example of the temperature changes at one nucleation site when in neighborhood there is located another nucleation site. We can notice that for temperature fluctuation shown in Fig. 3a,b,c,e, we can distinguish at least two kinds of changes. The first one is a temperature changes with high frequencies and low amplitude. The other one is a change with low frequencies and high amplitude. The examples of two kinds of temperature changes have been denoted by numbers 1 and 2 in Fig. 3a.

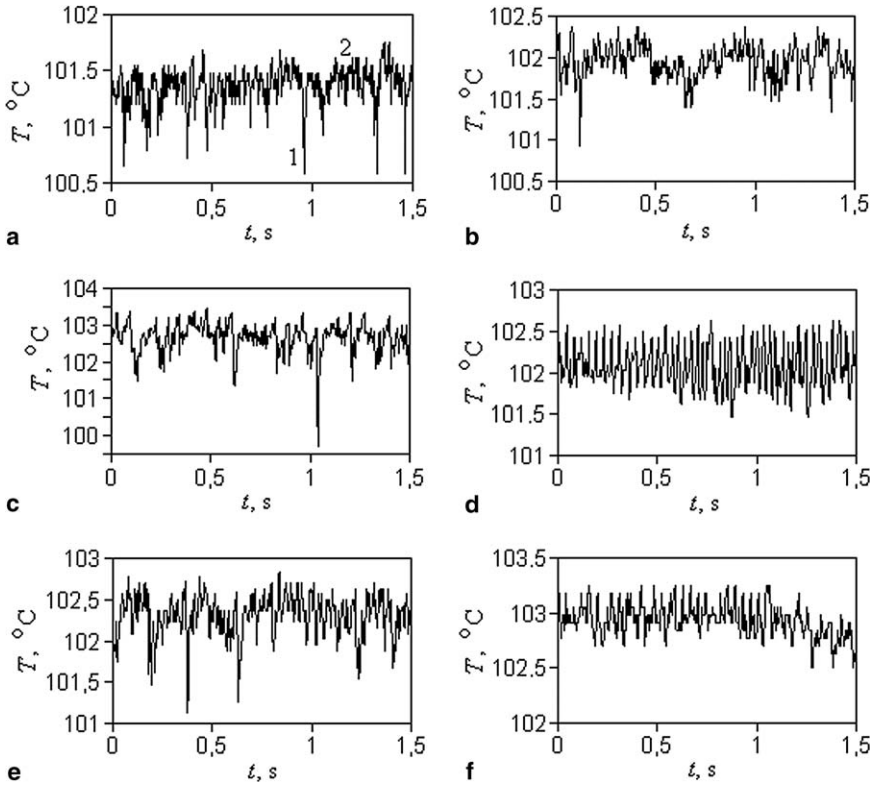

Fig. 3. Temperature changes under the cavities for different distance between neighboring cavities ($q = 26.5$ kW/m^2) for S/D equal to (a) 0.42, (b) 0.83, (c) 1.25, (d) 1.67, (e) 2.50, (f) 3.33 mm.

The number 1 indicates the high amplitude and number 2—the low amplitude of temperature changes. The different situations appear in cases shown in Fig. 3d,f for S/D equal to 1.67 and 3.33. In these both situations the temperature changes are rather similar to temperature changes at the single cavity.

In Fig. 4, the examples of wavelet power spectrum from the temperature changes at one of two neighboring cavities has been presented. The gray area indicates the maximum value of $|W(t,s)|^2$. The location of gray area show the changes of dominant frequencies of temperature fluctuation. In all cases under consideration the wavelet power spectrums are different from this one presented in Fig. 2c. During the cavity interaction it is impossible to identify the constant frequency of temperature changes at cavity. The gray areas shown in Fig. 4 are fragmented and located in place of low frequencies. As it has been mentioned above, the temperature changes with low frequency are connected with changes of conditions of heat transfer around the departing bubbles. Therefore in case under consideration the changes of location of gray area in Fig. 4 show the dynamic of conditions of heat transfer around the departing bubbles. In Fig. 4, we can distinguish the four types of wavelet power spectrums.

- The wavelet power spectrums shown in Fig. 4a,c,e for cavities distance equal to $S/D = 0.42$, $S/D = 1.25$, $S/D = 2.50$ characterize the relatively large fragmentation of the gray area. It means that the large temporary change of conditions of heat transfer around the bubbles emitted from twin cavities happens in these cases.
- In Fig. 4b for $S/D = 0.83$, the gray area is less fragmented than in Fig. 4a,c,e and located in the area of low frequencies. It is impossible to identify the frequency of bubbles departure. It means that in this case the conditions of heat transfer around the bubbles change less rapidly than in other cases.
- In Fig. 4d for $S/D = 1.67$, the gray area is fragmented but the maximums of wavelet power spectrum are located in the area of frequency about 30 Hz. In this case the temperature changes under the cavity become similar to temperature changes under the single cavity.
- The wavelet power spectrum shown in Fig. 4f is flat compared with power spectrums shown in other figures. It is impossible to identify the frequency of bubbles departure. The wavelet power spectrum is still different from this one shown in Fig. 2c under the single cavity. It means that the bubbles still weakly interact.

5. Analysis of cavities interaction

In order to understand the mechanism of interaction between cavities it is necessary to carry out the comparison of temperature time series recorded in both cavities. The correlation between time series can be calculated using the correlation coefficient, which is defined as follows [17]:

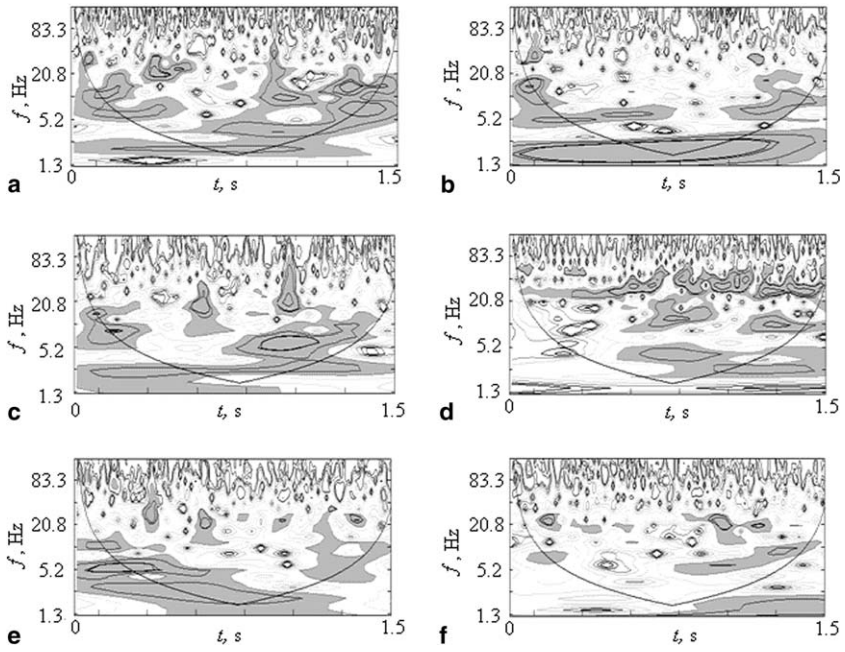

Fig. 4. The wavelet power spectrum of temperature fluctuation at one of two neighboring cavities ($q = 26.5$ kW/m^2), for S/D equal to (a) 0.42, (b) 0.83, (c) 1.25, (d) 1.67, (e) 2.50, (b) 3.33 mm. (Wavelet software was provided by Torrence and Compo, and is available at URL: http://paos.colorado.edu/research/wavelets/ [11,14].)

$$C_t = \frac{\mathrm{Cov}[T^{\mathrm{l}}(t), T^{\mathrm{r}}(t)]}{\sigma_{T^{\mathrm{l}}}\sigma_{T^{\mathrm{r}}}} \tag{5}$$

where T^{l} and T^{r} are time series of temperature measurements at left and right nucleation sites; σ_T^{l} and σ_T^{r} are the standard deviations of time series T^{l} and T^{r} respectively.

When $|C_t|$ is close to 1, time series T^{l} and T^{r} are correlated. When the large values in both series appear at the same time, then $C_t > 0$; but when large values in first series meet low values in other series, then $C_t < 0$. When C_t is close to zero, then the time series T^{l} and T^{r} are not correlated. The changes of value of coefficient C_t against spacing S/D is shown in Fig. 6.

Wavelet power spectrum allows us to observe changes in time of the power of all frequencies. Therefore we can use the wavelet power spectrum, prepared for data from interacting cavities, to identify the time correlation between the powers of frequencies of temperature fluctuation at neighboring cavities. For that purpose the following coefficient has been constructed:

$$C_f(s) = \frac{\mathrm{Cov}[|W^{\mathrm{l}}(t,s)|^2, |W^{\mathrm{r}}(t,s)|^2]}{\sigma_{|W^{\mathrm{l}}|^2}\sigma_{|W^{\mathrm{r}}|^2}} \tag{6}$$

where $|W^{\mathrm{l}}(t,s)|^2$ and $|W^{\mathrm{r}}(t,s)|^2$ are time series of wavelet power for the given value of parameter s at left and right cavities; $\sigma_{|W^{\mathrm{l}}|^2}$, $\sigma_{|W^{\mathrm{r}}|^2}$ are the standard deviations of time changes of wavelet power spectrum for the given value of parameter s.

The coefficient of correlation of time changes of wavelet power spectrum for the given frequency (value of parameter s), C_f, is a measure of frequencies synchronization in interacting cavities. When C_f is close to 1, then the considered frequency appears in both time series in the same moment of time. When C_f is close to -1, then the considered frequency appears in one time series and disappears in another time series in the same moment of time. In Fig. 5, it has been shown the values of coefficient C_f against frequencies for different distances between twin cavities. The values of coefficient C_f calculated for all frequencies of temperature changes (used for construction of wavelet

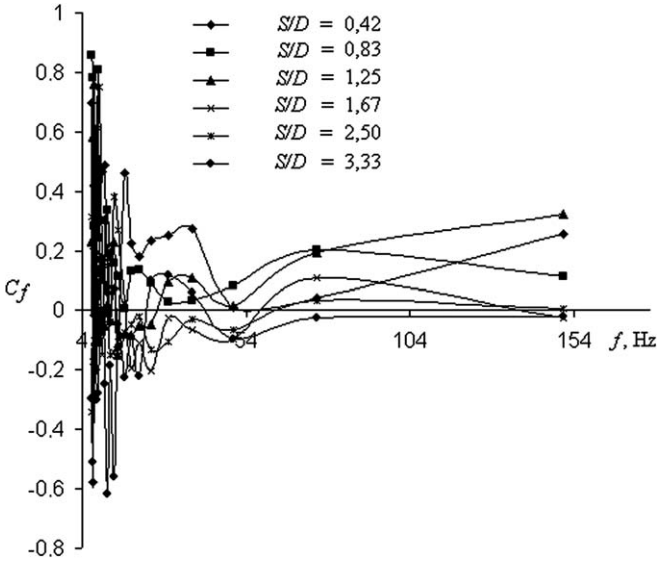

Fig. 5. Coefficient C_f of correlation of time changes of wavelet power spectrum for the given value of parameter s for different distance between twin cavities. For S/D equal to 0.42, 0.83, 1.25, 1.67, 2.50, 3.33 mm. $q = 26.5$ kW/m^2.

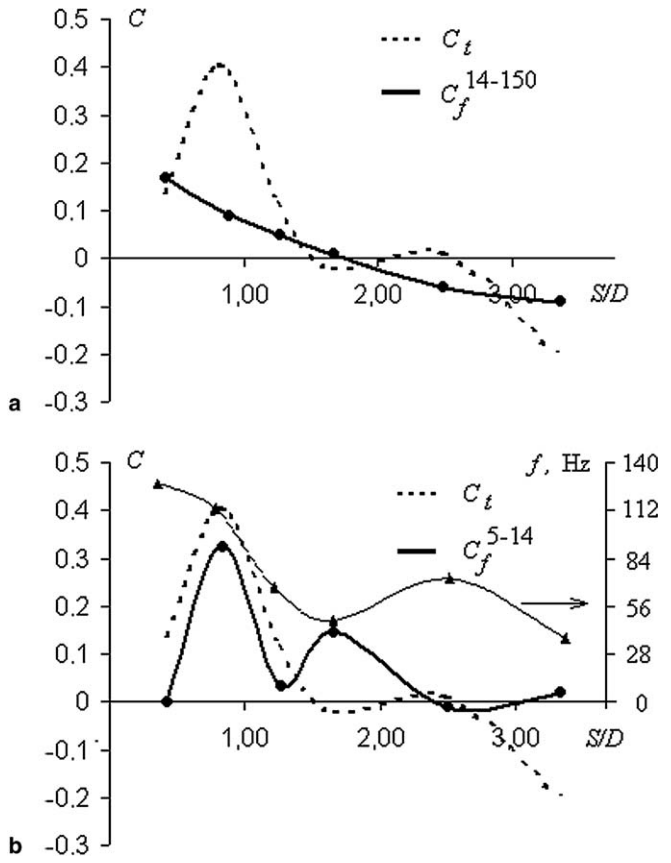

Fig. 6. Comparison of average values of coefficient C_f for different ranges of frequencies with coefficient C_t against different distance between twin cavities. For S/D equal to 0.42, 0.83, 1.25, 1.67, 2.50, 3.33 mm. $q = 26.5\ \mathrm{kW/m^2}$. (a) coefficient $C_f^{15\text{–}150}$ Hz, (b) coefficient $C_f^{5\text{–}14}$ Hz.

power spectrum) have a large scatter for low frequencies. The largest values of C_f and the largest fluctuation of C_f appear for frequencies less than 14 Hz. The mean frequency of bubble departure from twin cavities for $q = 26.5\ \mathrm{kW/m^2}$ ranges from 25 to 60 Hz [16]. The large frequency of bubble departure appears for distance equal to 2 mm while the small frequency appears for distance equal to 8 mm.

Because of large oscillations of values of coefficient C_f it is difficult to conduct the physical interpretation of obtained results using the curves shown in Fig. 5. Therefore the average values of coefficient C_f obtained for two ranges of frequencies have been calculated. It has been assumed that temperature changes with frequencies greater than 15 Hz are generated by processes of heat transfer directly connected with dynamic of bubbles growth, while the temperature changes with frequencies less than 15 Hz are generated by changes of heat transfer conditions around the cavities and departing bubbles. Therefore two ranges of frequencies have been considered: the first one from 5 to 14 Hz and the other one from 15 to 150 Hz.

The average coefficient of C_f calculates the average correlation between two wavelet power spectrums for frequencies from the given range. Another words we can say that the average value of coefficient C_f is a measure of correlation between the changes of average amplitude of frequencies from the given range in two time series. When $C_f > 0$ (for the given range of frequencies) then we can conclude that the increase of average amplitude of frequencies from the given range in one time series is accompanied by increase of average amplitude in another time series. When the average coefficient $C_f < 0$ then we can conclude that the increase of average amplitude of frequencies is accompanied by decrease of average amplitude in another time series. From this point of view we can conclude that the average value of coefficient C_f identifies the way of synchronization of frequencies from the range under consideration.

In Fig. 6, the comparison between the averages values of: coefficient C_f calculated for two ranges of frequencies under consideration and coefficient C_t against distance between twin cavities has been presented.

For $S/D < 1.5$ the values of coefficient C_t are greater than zero. It means that the increase of temperature at one cavity is connected with increase of temperature at neighboring cavity. The maximum values of coefficient C_t appear for $S/D = 0.83$. In this case the temperature changes at twin cavities are strongly correlated. This process is connected with formation of large bubble over the twin cavities. In the range of $1.5 < S/D < 2.5$ the values of coefficient C_t is close to zero, it means that the values of temperature changes are not correlated. For $S/D > 2.5$ the values of coefficient C_t is less than zero, it means that the increase of the temperature at one cavity is accompanied by decrease of temperature at the neighboring cavity. The changes of correlation coefficient calculated for temperature changes at different points on heating surface have been discussed in the paper [16].

In Fig. 6a, it has been shown the comparison of values of coefficient C_t and average values of coefficient $C_f^{15\text{–}150}$ obtained for frequencies from the range $15\ \mathrm{Hz} < f < 150 <$ Hz. The values of coefficient $C_f^{15\text{–}150}$ identify the synchronization of frequencies of temperature changes generated by processes appears directly over the neighboring cavities. For $S/D < 1.67$ the value of coefficient $C_f^{15\text{–}150}$ is greater then zero it mean then the increase of frequencies of temperature changes at one cavity is accompanied by increase of frequencies of temperature changes at the neighboring cavity. From this point of view we can conclude that for $S/D < 1.67$ the increase of activity of one cavity promote the activity of another cavity. Analysis of video films shows that for $S/D \approx 1.5$ the coalescence process disappears and the process of hydrodynamic interaction between the departing bubbles begins. Therefore, we can conclude that the process of synchronization of frequencies of temperature changes at cavities is connected with coalescent process. For $S/D > 1.67$ the values of $C_f^{15\text{–}150}$ is negative, which means that increase of average frequencies amplitude of temperature changes in one cavity is correlated with decrease of average frequencies amplitude of temperature changes in neighboring cavities. From

this point of view we can conclude that for $S/D > 1.67$ the activity of one cavity inhibits the activity of another cavity.

Fig. 6b presents the average value of coefficient C_f^{5-14} calculated for frequencies of temperature changes in range of 5 Hz $< f <$ 14 Hz. The changes of coefficient C_f^{5-14} shown in Fig. 6b are characteristic for processes connected with changes of condition of heat transfer around the twin cavities and departing bubbles. The function C_f^{5-14} has two maximums. The first one for $S/D = 0.83$ are connected with formation of large bubble over the twin cavities. This process leads to unification of the condition of heat transfer over the twin cavities and to synchronization of temperature changes at cavities. When coalescence disappears the coefficient C_f^{5-14} reaches the minimum value for $S/D = 1.25$. The disappearance of bubbles coalescence causes that the condition of heat transfer over each cavity becomes independent—frequencies of temperature changes at cavities become not synchronized. The increase of distance between cavities causes the increase of value of coefficient C_f^{5-14}. The coefficient C_f^{5-14} reaches the second local maximum for $S/D = 1.67$. For the same distance, the temperature changes occurring with high frequencies at neighboring cavities become independent (Fig. 6a). In this case the conditions of heat transfer around the cavities become unified. We can expect that this process is a consequence of hydrodynamic interaction between departing bubbles, but because of relatively large distance between cavities the thermal interaction is too small to synchronize the bubble growth dynamic, therefore the coefficient C_f^{15-150} is close to zero.

6. Modeling

The temperature changes of heating surface recorded in the experiment are created by heat transfer within the heating surface, liquid and vapor as well by liquid movement and phase changes. The cavity interaction through the heat transfer in heating surface has been investigated in the paper [12]. In the present study, the slightly modified model proposed by Yanagita [19,20] and Shoji [21] has been used to study the behavior of cavities and departing bubbles interaction.

The boiling on a thin and horizontal heating surface has been considered. Two-dimensional boiling field was approximated and modeled using CML method, where dynamic processes are formulated as difference equations. In the boiling models [19–21], it has been assumed that boiling is governed by the following processes: thermal diffusion, bubble rising and motion, thermal convection and phase change.

In the present study, the two-dimensional boiling field was divided into 21×19 rectangular lattices. Each lattice was marked by horizontal and vertical indexes, j and i. The lattices for $j = 0$ and $j = -1$ are located in the heating surface and the lattices for $j = 1$–19 are located in the liquid. On the heating surface two nucleation sites have been located. The schematic drawing of lattice under consideration has been shown in Fig. 7.

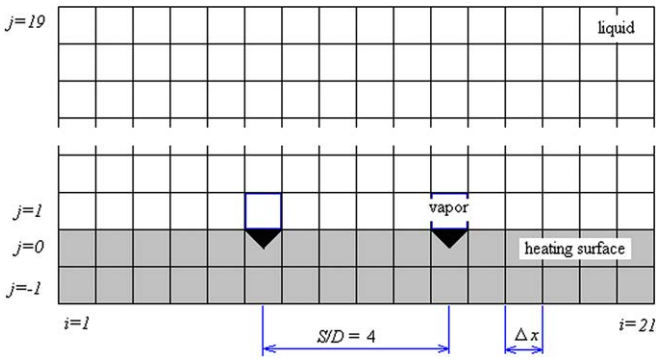

Fig. 7. Schematic drawing of lattice.

From the finite difference expression of heat conduction equation, the following mapping for thermal diffusion in the liquid, vapor and heating surface has been used [19,20]:

$$T' = T_{ij} + \frac{\varepsilon}{4}(T_{i+1,j} + T_{i-1,j} + T_{i,j+1} + T_{i,j-1} - 4T_{ij}) \tag{7}$$

where ε is a parameter representing the thermal diffusion, $\varepsilon = 4\alpha\Delta t/\Delta x^2$ [21], Δx is the size of the lattice and Δt is the time increment corresponding to one step of mapping.

The bubble motion due to buoyancy and its effect on temperature has been expressed by the following mapping [21]:

$$T''_{ij} = T'_{ij} + \frac{s_{ij}}{2}(\rho_{i,j+1} - \rho_{i,j-1})T'_{ij} \tag{8}$$

where $\rho = 1$ for liquid and $\rho = 0$ for vapor and s_{ij} is a parameter representing the velocity of bubble rising and the thermal convection. $s_{ij} = \frac{(\Delta t)^2}{\Delta x} g \frac{(T_\infty - T)}{T_{sat}}$ [21].

It has been assumed that the latent heat is consumed when liquid evaporates and released when vapor condenses. This phase change process was formulated as follows [21]:

$$\begin{aligned} &\text{for liquid, when } T''_{ij} \geqslant T_{\mathrm{cf}}; \quad T''_{ij} = T''_{ij} - \eta \\ &\text{for vapor, when } T''_{ij} < T_{\mathrm{cf}}; \quad T''_{ij} = T''_{ij} + \eta \end{aligned} \tag{9}$$

The simulation has been carried out for different spacing between twin cavities. The initial conditions for each simulation were the same. The liquid had the constant initial temperature equal to 99, 95 °C. The temperature of heating surface for $j = -1$ was equal to 101 °C + δ, where δ was a random value from range $(-0.1, 01)$. The temperature of phase change was equal to 100 °C. During the calculation procedure the subsequent values of temperatures was calculated according to Eqs. (7)–(9).

For simulation of process of cavities interaction two models have been considered.

- In the first model it has been assumed that bubbles can be created in liquid only over the cavities. In this case the condition (9) has a form

for liquid over the cavity, when $T''_{ij} \geqslant T_{cf}$; $T''_{ij} = T''_{ij} - \eta$,
for vapor over the cavity, when $T''_{ij} < T_{cf}$; $T''_{ij} = T''_{i1} + \eta$,
for liquid not over the cavity $T''_{ij} = T''_{ij}$.

(10)

In this case the bubble departure from twin cavities interacts only by heat conductivity between bubble columns.

- In the other model it has been assumed that in the first liquid layer (for $j = 1$) the bubbles can be created only over the cavities but for another liquid layers (for $j > 1$) the vapor can be created both over the cavities and in cells located between the cavities. The possibility of vapor creation in liquid located between cavities simulates the bubble motion and thermal convection between bubble columns. In this case the bubbles departing from cavities interact through thermal and hydrodynamic way. In the considered case, the condition (9) has a form:

for liquid over the cavity, when $T''_{ij} \geqslant T_{cf}$; $T''_{ij} = T''_{ij} - \eta$
for vapor over the cavity, when $T''_{ij} < T_{cf}$; $T''_{ij} = T''_{ij} + \eta$
for liquid between the cavities for $j > 1$,
when $T''_{ij} \geqslant T_{cf}$; $T''_{ij} = T''_{ij} - \eta$
for liquid between the cavities for $j > 1$,
when $T''_{ij} < T_{cf}$; $T''_{ij} = T''_{ij} + \eta$
for other cells containing liquid $T''_{ij} = T''_{ij}$

(11)

In both models, the temperature of heating surface for $j = 0$ at the cavities has been recorded after first 2000 iterations when stationary state has been obtained in the system. It has been assumed that in the model under consideration the diameter of departing bubble is equal to Δx. The example of temperature changes at twin cavities with spacing equal to $S/D = 3$ has been shown in Fig. 8. The temperature changes are chaotic. The mechanism of

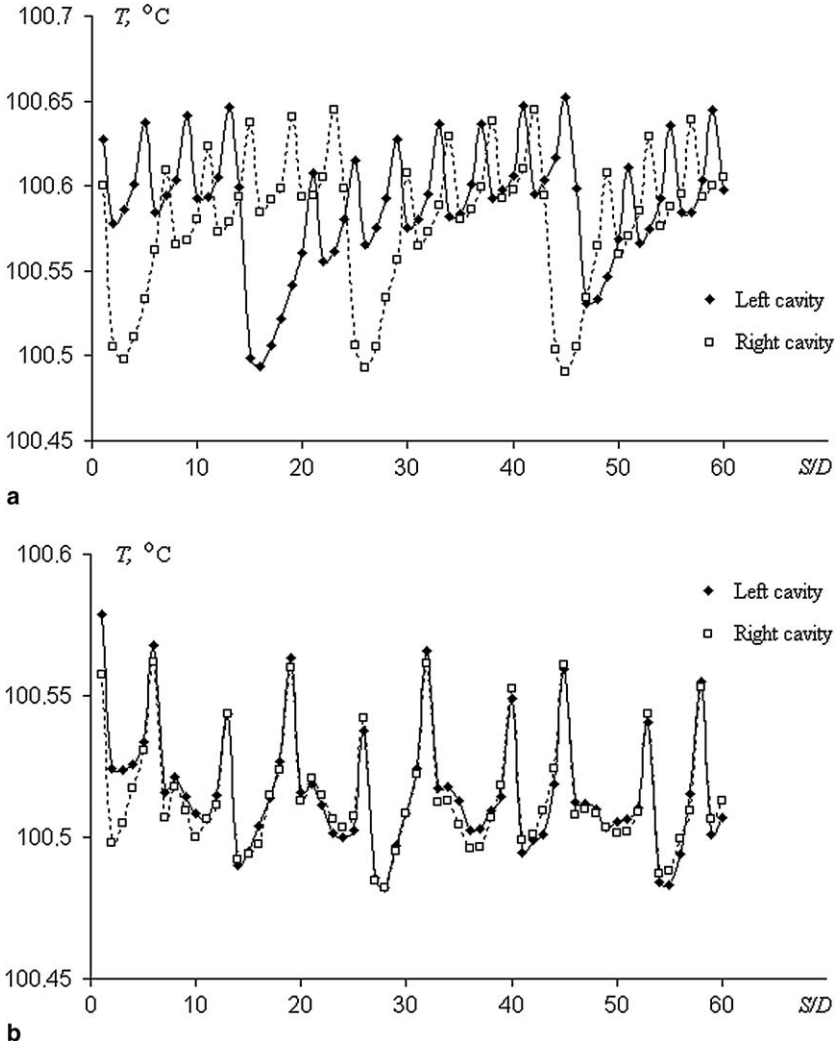

Fig. 8. Temperature changes at twin cavities for $S/D = 3$. Calculation has been made for $\varepsilon = 0.4$, $T_{cf} = 100$ °C, $s_{ij} = 0.015$, $\eta = 1$, temperature of heating surface was equal to 101 °C. (a) The bubbles can be created in liquid only over the cavities, (b) in the first liquid layer (for $j = 1$) bubbles can be created only over the cavities but for another liquid layers (for $j > 1$) vapor can be created both over the cavities and in cells located between cavities.

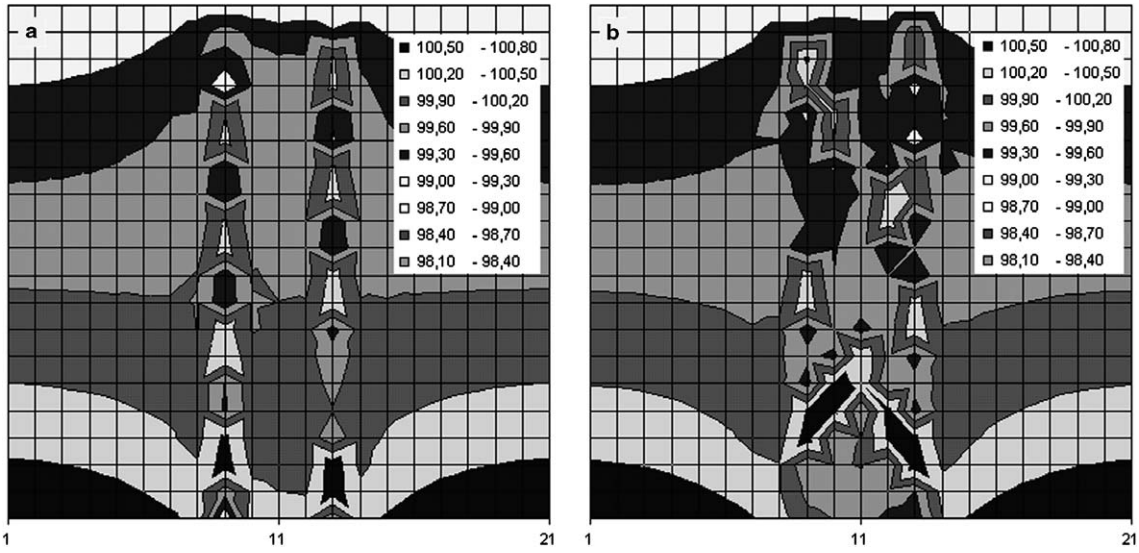

Fig. 9. The example of temperature field in liquid in two considered models for $S/D = 3$. Calculation has been made for $\varepsilon = 0.4$, $T_{cf} = 100$ °C, $s_{ij} = 0.015$, $\eta = 1$, temperature of heating surface was equal to 101 °C. (a) The bubbles can be created in liquid only over the cavities, (b) in the first liquid layer (for $j = 1$) bubbles can be created only over the cavities but for another liquid layers (for $j > 1$) vapor can be created both over the cavities and in cells located between cavities.

chaos appearance in system under consideration was discussed in the papers [19,20], therefore at present this problem was omitted. In Fig. 9, it has been shown the example of temperature field in boiling liquid, obtained during the simulation in both models under considerations. In Fig. 9b, it is visible the modification of temperature field by hydrodynamic interaction between bubble columns.

For different cavities spacing the correlation coefficient between temperatures of heating surface at cavities has been calculated. In Fig. 10, the comparison between the experimental results and results obtained from the models under consideration has been shown.

In case of first model (thermal interaction), when distance between the cavities is less than 1.5, the bubbles depart from both cavities at the same time. The correlation coefficient decreases together with increase in the spacing between the cavities. Generally, for $1.5 < S/D < 2.75$, when bubble is over the one cavity in the same time there is a liquid over another cavity. In the spacing range of $2.75 < S/D < 5$, the correlation between temperatures changes is low, this means that the cavities become independent. The qualitative accordance between the model and experimental results has been obtained for $S/D < 2$.

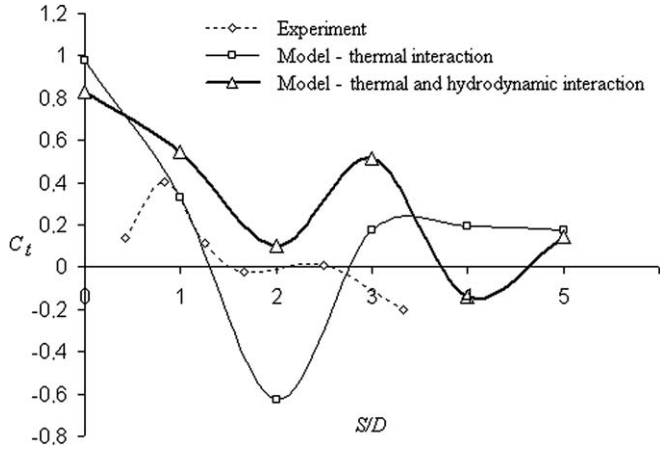

Fig. 10. Correlation coefficient between time series of heating surface temperature at twin cavities against cavities spacing, $\varepsilon = 0.4$, $T_{cf} = 100$ °C, $s_{ij} = 0.015$, $\eta = 1$ for second model and $\eta = 0.5$ for first model, temperature of heating surface equal to 101 °C.

The hydrodynamic interaction between two bubble columns increases the correlation between temperature changes at twin cavities. For $S/D = 2$ the correlation coefficient reaches the minimum, but its value is negative. For $S/D = 3$ the correlation coefficient reaches the positive maximum and for $S/D = 4$ it becomes negative. The obtained result is similar to results obtained from the experiment.

7. Conclusion

The analysis of correlation between the wavelet spectrums of low frequencies of temperature changes under twin cavities shows, that the process of bubbles departure can be synchronized and create the unified condition for heat transfer around the cavities for $S/D = 0.83$—in the coalescence process and for $S/D = 1.67$—in the hydrodynamic interaction between departing bubbles. For the other distances the conditions of heat transfer around the cavities are not unified. The coefficient C_f^{5-14} identifies also the distance for which the coalescence becomes not intensive, it happens for $S/D = 1.25$. Analysis of correlation between the high frequencies of temperature changes at the twin cavities allows us to define the distance between the cavities for which the direct thermal interaction between the neighboring cavities disappears. It happens for $S/D = 1.67$.

The wavelet power spectrum shows that even for the large distance between the bubbles (equal to 8 mm) the changes of temperature at neighboring cavities are different from these ones obtained for single cavity. Therefore, we can conclude that the process of bubbles growth is sensitive to small changes of conditions of heat and mass transfer around the bubbles. The discovery of the existence of maximum of coefficient C_f^{5-14} for $S/D = 1.67$ confirms the existence of phenomenon of synchronization of bubbles dynamic through liquid flow induced by departing bubbles. The values of C_f^{15-150} allows us to formulate the new answer to the question of promotion and inhibition of interacting nucleation sites. It has been found out that for $S/D < 1.67$ the increase of activity of one cavity promotes the activity of another cavity, and for $S/D > 1.67$ the activity of one cavity inhibit the activity of another cavity.

The carried out simulation shows that thermal interaction between two cavities and bubble columns leads to deactivation of neighboring cavity. The hydrodynamic interaction sustains the activity of neighboring cavities and for larger distance contradicts to effect of thermal cavity deactivation process. After decrease of thermal interaction (during the spacing increase) the hydrodynamic interaction leads to cavity correlation for $S/D = 3$ in the model (Fig. 10).

Acknowledgement

The authors would like to express their appreciation to Dr. Lei Zhang, for her contribution in performing the experiment.

References

[1] R.L. Judd, On nucleation site interaction, J. Heat Transfer 110 (1988) 475–478.
[2] D.M. Qiu, V.K. Dhir, Single bubble dynamics during nucleate boiling under low gravity conditions, in: Engineering Foundation Conference on Microgravity Fluid Physics and Heat Transfer, Hawaii, 1999, pp. 61–71.
[3] V.V. Chekanov, Interaction of centers in nucleate boiling, Teplofzika Vysokikh Temperaur 15 (1977) 121–128.
[4] A. Calka, R.L. Judd, Some aspects of the interaction among nucleation sites during saturated nucleate boiling, Int. J. Heat Mass Transfer 28 (1985) 2331–2342.
[5] H. Gjerkeš, I. Golobic, Measurement of certain parameters influencing activity of nucleation sites in pool boiling, Exp. Thermal Fluid Sci. 25 (2002) 487–493.
[6] H. Kubo, H. Takamatsu, H. Honda, Effects of size and number density of micro-reentrant cavities on boiling heat transfer from a silicon chip immersed in degassed and gas-dissolved FC-72, Enhan. Heat Transfer 6 (1999) 151–160.
[7] S.H. Bhavnani, G. Fournelle, R.C. Jaeger, Immersion-cooled heat sinks for electronics: insight form high-speed photography, IEEE Trans. Comp. Packag. Technol. 23 (2001) 166–176.
[8] L. Zhang, M. Shoji, Nucleation site interaction in pool boiling on the artificial surface, Int. J. Heat Mass Transfer 46 (2003) 513–522.
[9] Y. Takagi, M. Shoji, Boiling features from a single artificial cavity, Int. J. Heat Mass Transfer 44 (2001) 2763–2776.
[10] J.H. Ellepola, D.B.R. Kenning, Nucleation site interactions in pool boiling, in: Second European Thermal-Sciences and 14th UIT National Heat Transfer Conference, 1996, pp. 1669–1675.
[11] C. Torrence, G.P. Compo, A Practical Guide to Wavelet Analysis, with Significance and Confidence Testing, 2005. Available from: <http://paos.colorado.edu/research/wavelets/>.
[12] R. Mosdorf, M. Shoji, Chaos in nucleate boiling—nonlinear analysis and modelling, Int. J. Heat Mass Transfer 47 (6–7) (2004) 1515–1524.
[13] R. Mosdorf, The mechanism of generation of chaotic fluctuation of heating surface temperature in nucleate boiling, Trans. Instit. Fluid-Flow Mach. 111 (2002) 1–17.
[14] C. Torrence, G.P. Compo, A practical guide to wavelet analysis, Bull. Am. Meteorolog. Soc. 79 (1) (1998).
[15] D.B.R. Kenning, Youyou Yan, Pool boiling heat transfer on a thin plate: features revealed by liquid crystal thermography, Int. J. Heat Mass Transfer 39 (15) (1996) 3117–3139.
[16] M. Shoji, R. Mosdorf, L. Zhang, Y. Takagi, K. Yasui and M. Yokota, Features of boiling on an artificial surface—bubble formation, wall temperature fluctuation and nucleation site interaction, in: First International Symposium on Thermal Science and Engineering, Beijing, China, October 23–26, 2002, pp. G293–302.
[17] L. Gajek, Wnioskowanie statystyczne, modele i metody, WNT, Warszawa, 2000 (in Polish).
[18] B.Staniszewski. Wymiana ciepła podstawy teoretyczne. PWN, Warszawa 1979 (in Polish).
[19] T. Yanagita, Phenomenology of boiling: a coupled map lattice model, Chaos 2 (3) (1992) 343–350.
[20] T. Yanagita, Coupled map lattice model for boiling, Phys. Lett. A 165 (5–6) (1992) 405–408, 1 June.
[21] M. Shoji, Boiling simulator: a simple theoretical model of boiling, A Keynote Article at the ICMFV8 (3rd International Conference of Multiphase Flow), June 8–12, Lyon, 1998.